Original article

Swertia chirayita suppresses the growth of non-small cell lung cancer A549 cells and concomitantly induces apoptosis via downregulation of JAK1/STAT3 pathway

Afza Ahmad [a], Rohit Kumar Tiwari [a], Tahani M. Almeleebia [b], Majed Saad Al Fayi [c], Mohammad Y. Alshahrani [d,c], Irfan Ahmad [c], Mohammad S. Abohassan [c], Mohd Saeed [e,*], Irfan Ahmad Ansari [a,*]

[a] *Department of Biosciences, Integral University, Kursi Road, Lucknow, Uttar Pradesh 226026, India*
[b] *Department of Clinical Pharmacy, College of Pharmacy, King Khalid University, P.O. Box 61413, Abha 9088, Saudi Arabia*
[c] *Department of Clinical Laboratory Sciences, College of Applied Medical Sciences, King Khalid University, P.O. Box 61413, Abha 9088, Saudi Arabia*
[d] *Research Center for Advanced Materials Science (RCAMS), King Khalid University, P.O. Box 9004, Abha 61413, Saudi Arabia*
[e] *Department of Biology, College of Sciences, University of Hail, Hail, Saudi Arabia*

A R T I C L E   I N F O

A B S T R A C T

Lung carcinoma is the leading cause of cancer-related mortalities worldwide, and present therapeutical interventions are not successful enough to treat this disease in many cases. Recent years have witnessed a surge in exploring natural compounds for their antiproliferative efficacy to expedite the characterization of novel anticancer chemotherapeutics. *Swertia chirayita* is a valued medicinal herb and possess intrinsic pharmaceutical potential. However, elucidation of its anticancer effects at molecular levels remains unclear and needs to be investigated. We assessed the anticancer and apoptotic efficacy of *S. chirayita* ethanolic extract (*Sw*-EtOH) on non-small cell lung cancer (NSCLC) A549 cells during this exploratory study. The results elucidated that *S. chirayita* extract induced toxic effects within lung cancer cells by ~1 fold during cytotoxicity and LDH release assay at a 400 μg/ml concentration. *Sw*-EtOH extract elevates the level of ROS, resulting in the disruption of $\Delta\psi$m and release of cytosolic cytochrome *c* by 3.15 fold. Activation of caspases-3, -8 & -9 also escalated by ~1 fold, which further catalyze the augmentation of PARP cleavage (~3 folds), resulting in a four-fold increase in *Sw*-EtOH induced apoptosis. The gene expression analysis further demonstrated that *Sw*-EtOH extracts inhibited JAK1/STAT3 signaling pathway by down-regulating the levels of JAK1 and STAT3 to nearly half a fold. Treatment of *Sw*-EtOH modulates the expression level of various STAT3 associated proteins, including Bcl-XL, Bcl-2, Mcl-1, Bax, p53, Fas, Fas-L, cyclinD1, c-myc, IL-6, p21 and p27 in NSCLC cells. Thus, our study provided a strong impetus that *Sw*-EtOH holds the translational potential of being further evaluated as efficient cancer therapeutics and a preventive agent for the management of NSCLC.

© 2021 Published by Elsevier B.V. on behalf of King Saud University. This is an open access article under the CC BY-NC-ND license (http://creativecommons.org/licenses/by-nc-nd/4.0/).

1. Introduction

According to the Global Cancer Observatory report, lung cancer cases constituted 18% of 18,078,957 cases during 2018 and were also responsible for 18.4% (1,761,007) fatalities, 9,555,027 casualties inclusive of different carcinomas (Taga et al., 1989). Lung cancer represents a serious cause of global health concern and is categorically delineated into small cell lung cancer and non-small cell lung cancer (SCLC/NSCLC), where the NSCLC is accountable for 80% of the cumulative lung cases (Ahmad et al., 2018; Darnell et al., 1994). Standard management of NSCLC relies on the stage at which the patient is diagnosed and commonly relies on the

* Corresponding authors.
    E-mail addresses: mo.saeed@uoh.edu.sa (M. Saeed), ahmadirfan.amu@gmail.com (Irfan Ahmad Ansari).
Peer review under responsibility of King Saud University.

Production and hosting by Elsevier

surgical removal of the tumor and radiotherapy or chemotherapy (Zappa and Mousa, 2016). Like in any other type of cancer, the chemotherapeutic intervention used to treat NSCLC has longer unavoidable side effects on the patients, therefore; reinforcing the urgent need for exploring safer options, namely the natural compounds to treat this debilitating disease (Yeh et al., 2013).

Natural compounds are currently being explored for their therapeutical potential in different types of carcinomas. One such traditional herb documented in Ayurvedic literature is *Swertia chirayita* belonging to the Gentianaceae family. *S. chirayita* is commonly found in sub-temperate regions of Himalayan bed ranging from Kashmir to Bhutan within an altitude range of 1200–2100 m and is also associated with names which usually differ in languages such as in Sanskrit the plant is referred to as Anaryatikta, Bhunimba, Chiratitka, Kairata whereas in Arabic and Farsi languages it is known as Qasabuzzarirah (Dutta et al., 2014; Yeh et al., 2013). Several scientific reports have earlier established that different extracts of *S. chirayita* have intrinsic antibacterial, antifungal, antiviral, anticancer, anti-inflammatory, antidiabetic and antioxidant characteristics (Kumar and Van Staden, 2015). However, no exhaustive study has been reported to decipher the molecular mechanism behind *S. chirayita* ethanolic extract on NSCLC of human origin, such as A549.

The JAK/STAT (Janus kinase /signal transducer and activator of transcription) pathway plays a crucial role during proliferation, inflammation, and tumour survival. JAK/STAT pathway is involved in the downstream activation of target genes upon stimulation with cytokines (IFN-α, IFN-β, IFN-γ), IL-6, along with growth factors, namely EGF and PDGF (Jin, 2020). Earlier reports have established an aberrant expression of the JAK/STAT pathway in various solid carcinomas such as head and neck, NSCLC and SCLC (LaFave and Levine, 2012). Enhanced activation of STAT3 is frequently reported in NSCLC and is further considered to play an imperative role in inducing cancer resistance towards standard and targeted molecular therapies (Yuan et al., 2019). STAT3 increases cancer cells' proliferation, migration, and survival and suppresses anti-cancer immune response (Yu et al., 2014).

Moreover, accumulating evidence has reported that upstream regulators of STAT3 play a vital role in lung cancer by augmenting the functional expression of IL-6 in about 40% of patients (Demaria et al., 2012). Subsequently, constitutive expression of JAK1/STAT3 is reported in cancerous cells and has been designated as a key pathway involved in the initiation and progression of cancer (Zhao et al., 2016). Consequently, JAK/STAT pathway is regarded as a promising target for exploring novel therapies. Owing to these attributes of the JAK1/STAT3 pathway, our present study was focused on elucidating the anticancer and antiproliferative effects of *S. chirayita* ethanolic extract on non-small human lung cancer A549 cells Fig. 1.

2. Materials

2.1. Reagents and chemicals

DAPI (4, 6-diamidino-2-phenylindole), propidium iodide (P.I.), and 2, 7-dichlorodihydrofluorescein diacetate (DCFH-DA) were purchased from Sigma (St. Louis, MO, USA). DMEM-high glucose, fetal bovine serum (FBS), 1% antibiotic–antimycotic solution, RNase A, HiPurATM Total RNA Miniprep Purification Kit and 3-(4, 5-dimethylthiazol-2-yl)-2,5-diphenyl tetrazolium bromide (MTT) were purchased from Himedia India, Ltd., Mumbai, India. Verso cDNA synthesis kit and DyNAmoColorFlash SYBR Green qPCR Kit were purchased from Thermo-Scientific, USA. FITC Annexin V Apoptosis Detection Kit was obtained from B.D. Bioscience, PharMingen (San Diego, CA, USA). Caspase-3, -8 and -9 activity

assay kits were purchased from BioVision, U.S.A. JC-1 mitochondrial membrane potential assay kit was purchased from G-Biosciences, USA. All the primer sequences utilized during the study were procured from IDT, USA.

2.2. Cell line maintenance

Human NSCLC cell line (A549) was obtained from the national repository division of the National Centre for Cell Sciences (NCCS), Pune, India. A549 cells were maintained in DMEM-high glucose enriched with 10% FBS along with 1% antibiotic-antimycotic solution. These cells were maintained under standard culture conditions at 37 °C in an atmosphere with at least 5% CO2.

2.3. Methods

2.3.1. Plant sample acquisition and preparation of S. chirayita ethanolic extract

S. chirayita whole plant was collected from the alpine area of district Pithoragarh in Uttarakhand, India, followed by its herbarium preparation. The whole plant parts of *S. chirayita* were preliminary washed with tap water, dried in the shed for nearly a week and later cut into small pieces for grinding in mortar and pestle. The obtained powdered form was stored in dry tubes. Subsequently, the powdered samples were packed in a Soxhlet apparatus and extracted with 70% ethanol at 60–65 °C for 4–5 h and subsequently sonicated (2 h). The extracted sample was filtered twice (Whatman No.1 filter), and the residual quantity of ethanol remaining within the extract was dried through evaporation under a vacuum. The resultant semi-solid ethanolic extract of *S. chirayita* (*Sw*-EtOH) was stored at 4 °C.

2.3.2. Evaluation of Sw-EtOH extract mediated toxicity on NSLC A549 cells

Sw-EtOH potential cytotoxic effects on A549 cells were determined using the previously-mentioned MTT assay with slight alterations (Tiwari et al., 2021). In brief, 5×10^3 A549 cells were seeded in each well of a 96-well plate and were treated with different *Sw*-EtOH concentrations (100, 200 and 400 μg/ml) for 24 h. Post incubation, media was replaced with MTT dye (5 mg/ml; 10 μl) and incubated for an additional four h. Post incubation, 100 μl of DMSO was added in each well to solubilize any formazan crystal (if formed). Eventually, the absorbance of formazan crystal was recorded at 570 nm through Bio-Rad, USA microplate reader. The viability of A549 cells treated with and without *Sw*-EtOH was expressed as cell viability percentage (%) by comparing the mean absorbance of cells from different groups as

Cell Viability (%) = (mean absorbance treated

$cells/meanabsorbanceuntreatedcells) \times 100$

To further substantiate *Sw*-EtOH mediated toxicity, lactate dehydrogenase (LDH) assay was performed using an LDH assay kit (Sigma-Aldrich, USA) as per the protocol described earlier (Lin et al., 2017). The LDH released by treated and untreated A549 cells was monitored by recording its absorbance at 490 nm using a microplate reader (Bio-Rad, USA). The LDH release at a different dosage of *Sw*-EtOH was stated in percentage (%) as

LDH release (%) = (mean absorbance treated

$cells/meanabsorbanceofuntreatedcells) \times 100$

2.3.3. Morphological assessment of A549 cells post-Sw-EtOH extract treatment

The morphological assessment of *Sw*-EtOH treated and untreated cells were additionally undertaken. Briefly, 10^4 cells
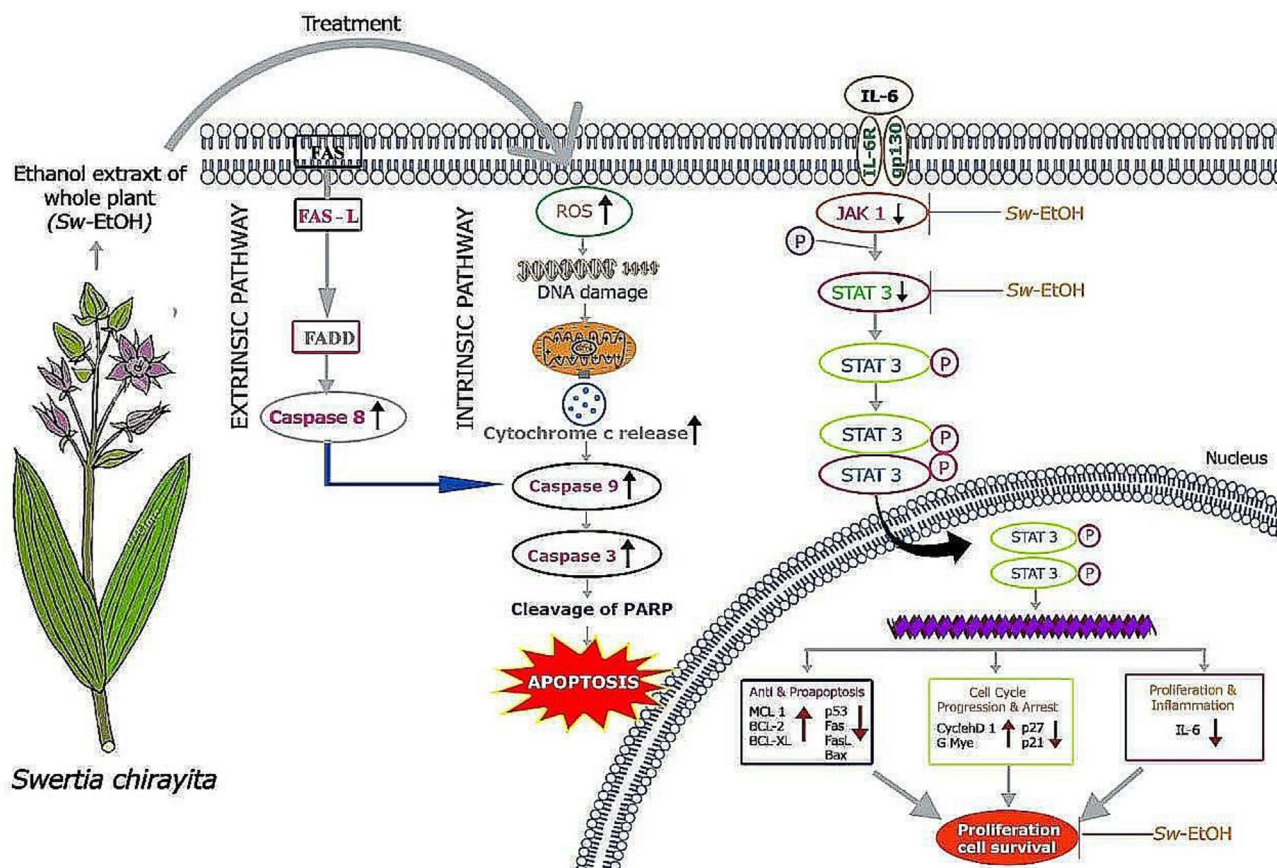
Fig. 1. Illustrative representation of *Swertia chirayita* mediated anti-proliferative effects on human non-small lung cancer A549 cells. *Sw*-EtOH was found to exert its anti-cancerous effects on A549 cells by impelling the extrinsic apoptotic pathway mediated by enhanced expression of caspase-8 enrouted to activation of Fas receptors by Fas-L. *Sw*-EtOH also indicated towards activation of intrinsic apoptotic pathway via augmentation of intracellular ROS levels concomitantly followed by increased levels of caspase dependent cleaved PARP protein. Furthermore, *Sw*-EtOH was also successful in modulating the JAK-STAT signaling pathway which eventually culminated in altered expression of signals required for cell survival and proliferation (as indicated by upwards and downwards arrow).

were seeded, dosed (with various *Sw*-EtOH concentrations) and incubated as per the protocol described in Section 2.3.2. After incubation, these treated cells were visualized to observe any changes in their appearance compared to the untreated control cells using FLoid Imaging Station, Thermo-Scientific, USA.

2.3.4. Assessment of Sw-EtOH extract-mediated oxidative stress within A549 cells

The efficacy of *Sw*-EtOH extract in instigating ROS within A549 cells was evaluated using DCFH-DA both qualitatively and quantitatively, as described earlier with slight modifications (Ahmad and Ansari, 2020). During qualitative assessment assay, 104 A549 cells were seeded in each well and treated with concentrations mentioned above of *Sw*-EtOH for six h. Subsequently, the respective wells stained with DCFH-DA (10 μM) for 30 min. The intensity of ROS-mediated fluorescence was assessed by differences within the intensity of green fluorescence (Channel excitation: emission ratio 482/18 nm: 532/59 nm) of the FLoid imaging station (Thermo-Scientific, USA).

2.3.5. Assessment of DNA damage in Sw-EtOH extract-treated A549 cells

Following the dosing schedule, as stated above in 96-well plate at varying *Sw*-EtOH concentration, 8-hydroxy-29-deoxyguanosine (8-OHdG) levels in A549 cells were investigated colorimetrically using OxiSelectTM Oxidative DNA Damage ELISA Kit (Cell Biolabs, Inc.) as per the manufacturer protocol.

2.3.6. Qualitative estimation of Sw-EtOH induced apoptosis

To qualitatively analyze *Sw*-EtOH induced apoptosis within A549 cells, double staining using DAPI and P.I. stain was performed. A549 cells were treated with stated concentrations of *Sw*-EtOH and incubated for 24 h. Fluorescent micrographs were then captured using FLoid Imaging station (Thermo-Scientific, USA) at blue (Excitation: Emission:390/40 nm:446/33 nm) and red filters (Excitation:Emission: 586/15 nm:646/68 nm).

2.3.7. Quantification of Sw-EtOH insinuated apoptosis through Annexin-V/FITC staining

To quantitatively assess the apoptosis induced in A549 cells post-*Sw*-EtOH treatment, Annexin V-FITC/PI apoptosis kit (B.D. Biosciences, USA) was used as described earlier (Wang et al., 2018). Briefly, 4X105 A549 cells/well were treated with different Sw-EtOH concentrations (100, 200 and 400 μg/ml) and incubated for 24 h. After incubation, the cells were washed (1X PBS) and treated with 1X binding buffer (as per manufacturers' protocol). Eventually, cells from each group were incubated with Annexin V-FITC, P.I. at R.T. in the dark for 15 min. The suspension was finally assessed through flow cytometry using FACS Calibur (B.D. Biosciences, USA).

2.3.8. Alterations in mitochondrial potential (ΔΨm) within A549 cells post-Sw-EtOH extract treatment

Alteration in ΔΨm in *Sw*-EtOH treated A549 cells was assessed qualitatively using JC-1. The cells treated with or without *Sw*-EtOH extract were incubated for 30 min with JC-1 stain (200 μM) before

visualization and image acquisition using red fluorescence filter of Floid imaging station (Thermo-Scientific, US; Excitation:586/15 nm: Emission:646/68 nm).

2.3.9. Cytochrome-c release assay

The cytochrome-c release assay was carried out as per the manufacturers' protocol described earlier (Chen et al., 2013). Briefly, 106 cells/well were co-cultured with different Sw-EtOH concentrations (100, 200 and 400 μg/ml) and incubated for 24 h. Further, the cells were centrifuged (1000 rpm; 10 min at 37 °C) and washed using ice-cold 1X PBS. Next, the total protein content of cells was obtained using T-PER Tissue Protein Extraction Reagent (ThermoFischer Scientific, U.S.). The presence of cytochrome-c within the total extracted protein of treated and untreated A549 cells was investigated using an ELISA kit (KHO1051; ThermoFischer Scientific, U.S.) following manufacturers' protocol.

2.3.10. Evaluation of caspase activity within Sw-EtOH extract-treated A549 cells

Colorimetric assay kits specific for caspase-8, -9 and -3 were used to determine the caspase activities in Sw-EtOH extract-treated human NSCLC A549 cells following the manufacturer's protocol. Percent (%) increase in the caspases activity was determined by comparing the result with the level of untreated A549 cells as control.

2.3.11. Evaluation of cleaved Poly (ADP-ribose) polymerase (PARP) levels post-Sw-EtOH extract treatment

Cleaved PARP levels within Sw-EtOH extract-treated A549 cells were assessed using a Human PARP ELISA using manufacturer's instruction. Cell absorbance from Sw-EtOH was recorded at 450 nm on a microplate reader (Bio-Rad, USA).

2.3.12. Real-time PCR (qPCR) analysis

Total RNA content of 106 A549 cells treated with and without Sw-EtOH was extracted through HiPurATM Total RNA Miniprep Purification Kit. Subsequently, isolated RNA (2 μg) was used to prepare cDNA using a Verso cDNA synthesis kit as per the manufacturer's protocol. The primers used during the assay were as described earlier (Cui and Placzek, 2016; Karagul et al., 2020; Lee et al., 2019; Medeiros et al., 2002; Rego et al., 2011; Shamloo and Usluer, 2019; Sun et al., 2020; Tao et al., 2020; Yang et al., 2012; Zucchini et al., 2005) and mentioned in Table 1. qPCR analysis was then undertaken on ABI-7500 real-time PCR (Applied Biosystems) by applying DyNAmoColorFlash SYBR Green qPCR Kit following the suppliers' protocol. The normalization of different

treatment groups was done against glyceraldehyde 3-phosphate dehydrogenase (GAPDH). The comparative C.T. method was employed to analyze the data, and fold change among treatment groups were estimated using the $2 - \Delta\Delta CT$ method.

3. Results

3.1. Sw-EtOH mediated cytotoxic effects within A549 NSCLC cells

This exploratory study initially investigated the cytotoxic and antiproliferative effects instigated by Sw-EtOH on human NSCLC A549 cells. The results affirmed that Sw-EtOH extract treatment inhibited the cell growth and proliferation of A549 lung carcinoma cells dose-dependently ($p < 0.001$), as shown in Fig. 2A. The dose-dependent inhibition of A549 cells after treatment with Sw-EtOH (100, 200 and 400 μg/ml) was found to be 86.07% ± 4.82, 55.88 ± 3.53% and 25.75 ± 5.58% respectively as compared to untreated control cells (Fig. 2A).

Similarly, LDH cytotoxicity assay was performed to test whether Sw-EtOH extract inhibited the proliferation of human NSCLC A549 cells. Further, A549 cells were treated with various doses (100–400 μg/ml) of Sw-EtOH extract for 24 h, LDH cytotoxicity was analyzed. As shown in Fig. 2B, Sw-EtOH extract strongly suppressed the viability of NSCLC cells in a dose-proportional manner ($p < 0.001$) and increased LDH release was observed to be 38.61 ± 3.54%, 57.38 ± 3.85% and 71.52 ± 4.75% at the above-stated concentrations of Sw-EtOH extract.

Moreover, alterations in the morphology of Sw-EtOH treated A549 NSCLC cells were studied by performing phase-contrast microscopy. We observed various morphological alterations such as cell shrinkage, swelling, cytoplasm and nuclear condensation, cell granulation, and withering of cell organelles indicated by pink, blue and orange arrows (Fig. 2C), suggesting dose-dependent Sw-EtOH mediated cytotoxicity in A549 NSCLC cells.

3.2. Sw-EtOH induces apoptosis in A549 NSCLC cells

Various cell-based apoptosis assays were undertaken to confirm whether the cytotoxic effect of Sw-EtOH extract on lung cancer cells was due to apoptosis. DAPI/PI double fluorescent staining was undertaken to investigate apoptotic cell death in A549 NSCLC cells post-Sw-EtOH treatment. As evident in Fig. 3A, a dose-dependent increase in the number of Sw-EtOH-treated A549 cells with bright blue and red nuclei (indicating apoptosis shown by red and green arrows), whereas the untreated A549 cells exhibited

Table 1
List of primers used for qPCR.

| S. No.	Target gene	Sequence of primers	
		Forward (5′-3′)	Reverse (3′-5′)
1.	GAPDH	GAAATCCCATCACCATCTTCCAGG	GAGCCCCAGCCTTCTCCATG
2.	Bcl2	GATTGTGGCCTTCTTTGAG	CAAACTGAGCAGAGTCTTC
3.	Bcl-X$_L$	CAGAGCTTTGAACAGGTAG	GCTCTCGGGTGCTGTATTG
4.	Mcl-1	GGACATCAAAAACGAAGACG	GCAGCTTTCTTGGTTTATGG
5.	c-myc	AGCGACTCTGAGGAGGAACAAG	GTGGCACCTCTTGAGGACCA
6.	Cyclin D1	CCGTCCATGCGGAAGATC	GAAGACCTCCTCCTCGCACT
7.	p53	CCCCTCCTGGCCCCTGTCATCTTC;	GCAGCGCCTCACAACCTCCGTCAT;
8.	p21	TCCAGGTTCAACCCACAGCTACTT	TCAGATGACTCTGGGAAACGCCAA
9.	p27	CCTCCTCCAAGACAAACAGCG	GGGCATTCAGAGCGGGATT
10.	Fas	CGGACCCAGAATACCAAGTG	CCAAGTTAGATCTG
11.	Fas-L	GGGG	GTGGCCTAT
		ATGTT TCAGCTCTTCC-3	TTG CTT CTCCA
12.	Bax	GCCCTTTTGCTTCAGGGTTT	TCCAATGTCCAGCCCATGAT
13.	JAK1	ATCCTTCGCACAGACAACATC	GCATTCCTGAGCCTTCTTGG
14.	STAT3	CTGGCCTTTGGTGTTGAAAT	AAGGCACCCACAGAAACAAC
15.	IL-6	GAC AAA GCC AGA GTC CTT CAG AGA G	CTA GGT TTG CCG AGTAGATCT C
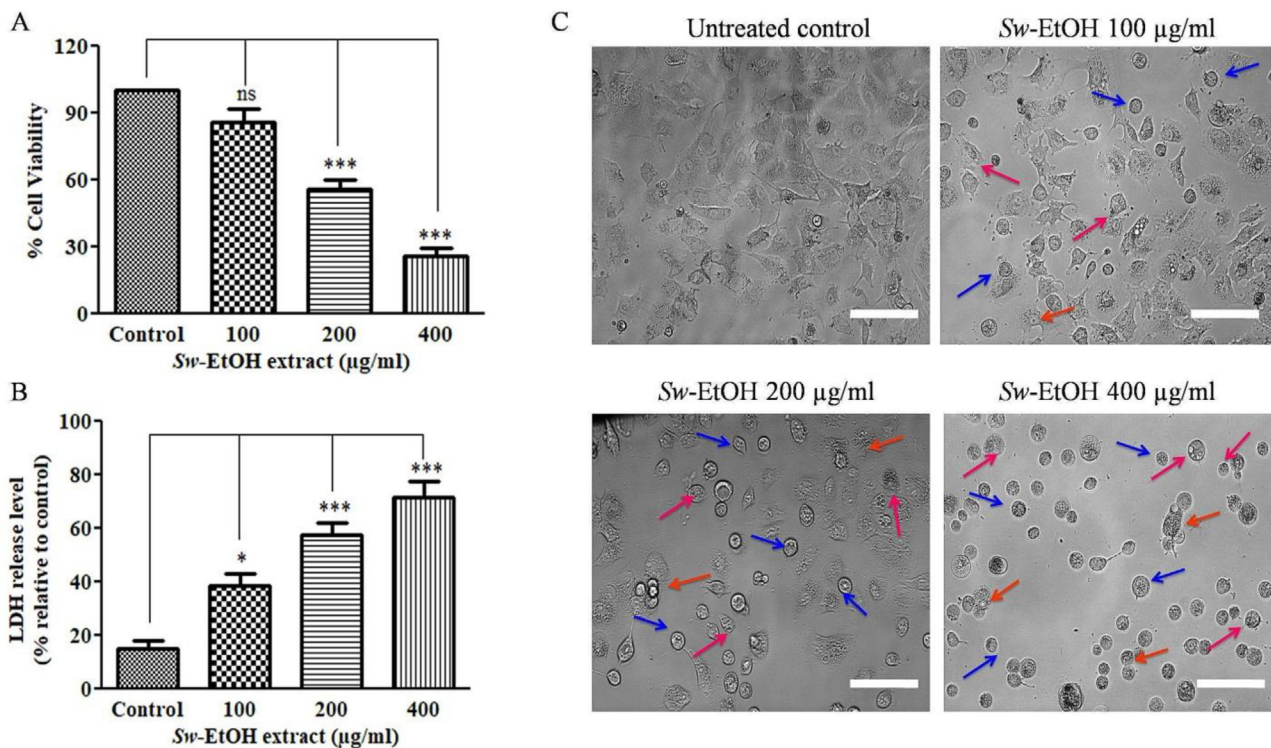
Fig. 2. *Sw*-EtOH induced cytotoxicity within human lung cancer A549 cells. (A) Percent (%) cell viability of A549 cells after *Sw*-EtOH treatment at concentrations of 100–400 μg/ml after 24 h, (B) assessment of membrane integrity as evaluated through LDH release assay at aforesaid dosage of *Sw*-EtOH and (C) Phase-contrast images of *Sw*-EtOH treated A549 cells for 24 h respectively (pink, blue and orange arrows indicate cell, shrinkage and withering of cell organelles). Data communicated constitutes the mean ± SEM of individual experiments performed thrice in triplicates. The level of significance among different *Sw*-EtOH treated groups was determined using one-way Anova and Dunnett post-hoc in comparison with untreated control where *represents $p < 0.05$, **$p < 0.01$ and ***$p < 0.001$; Scale bar = 100 μm.

diffuse blue and red nuclei (highly proliferating cells). Further, the merge fluorescence of DAPI/PI-stained cells was shown by white arrows demonstrating apoptosis in *Sw*-EtOH-treated lung cancer cells.

Furthermore, apoptosis was also assessed by Annexin-V FITC/PI assay to quantify the rates of apoptosis induced by *Sw*-EtOH treatment in A549 NSCLC cells. As observed in Fig. 3B, cells in the upper right quadrant (U.R.) undergo early-stage apoptosis (Annexin V-FITC +, P.I.−), and cells in the lower right quadrant (L.R.) witness late-stage apoptosis (Annexin V-FITC +, PI+) were referred to as apoptotic cells. The results exhibited that *Sw*-EtOH treatment increases dose-reliant apoptosis rates by 11.28 ± 3.74%, 16.53 ± 4. 41%, 27.76 ± 3.87%, 50.99 ± 4.14% and 58.86 ± 4.20% in A549 NSCLC cells ($p < 0.001$) (Fig. 3C).

3.3. Sw-EtOH instigated caspase apoptotic pathways in A549 NSCLC cells

To explore the fundamental mechanism involved in *Sw*-EtOH-mediated apoptosis in A549 NSCLC cells carcinoma cells, the intrinsic caspase pathway and extrinsic apoptosis pathway were initially studied, as shown in Fig. 4A, caspase-3, -8 & -9 activities were significantly increased by 64.36 ± 2.85%, 153.25 ± 2.63% and 206.38 ± 3.26%; 33.21 ± 3.12%, 119.06 ± 6.40% & 155.94 ± 4.73% and 50. 31 ± 5.16%, 128 ± 4.16% & 169.86 ± 4.81%, respectively as compared to the control after treatment with varying doses of *Sw*-EtOH ($p < 0.001$) (Fig. 4A).

Moreover, *Sw*-EtOH dose-proportionally induced the cleavage of PARP (2.74 fold; $p < 0.01$), which is a marker of apoptosis, coupled with an increased level of cytochrome *c* release ($p < 0.01$) in A549 NSCLC cells, thereby indicating the role of mitochondrial apoptotic pathway (Fig. 4B & 4C).

Loss of ΔΨm trigger off cytochrome *c* release from mitochondria to the cytosol, which is regarded as strong activators of the apoptotic caspase cascade. We, therefore, investigated the effect of *Sw*-EtOH on disruption in ΔΨm in JC-1 dye-stained A549 cells. The results demonstrated that *Sw*-EtOH treatment decreased ΔΨm in a dose reliant manner in A549 cells (Fig. 4D), substantiating the contribution of mitochondria in *Sw*-EtOH -induced apoptosis.

In addition, to decipher the mechanism of *Sw*-EtOH-induced apoptosis, we assessed the production of reactive oxygen species (ROS) (DCFH-DA staining. The fluorescent micrographs depicted that treatment of *Sw*-EtOH resulted in strong DCF-fluorescence intensity in A549 cells, stipulating an enhanced intracellular ROS generation (Fig. 4E). To further investigate whether DNA damage induced in *Sw*-EtOH extract-treated A549 lung cancer cells contributed to apoptosis induction. 8-OHdG, a product of oxidative damage to 2′-deoxyguanosine, is an established ubiquitous marker of oxidative imbalance induced by the generation of free radicals and is regarded as a critical attribute during carcinogenesis. It is physiologically formed and increased by anticancer agents (Kaushik et al., 2015). As observed in Fig. 4F, 8-OHdG was found to be substantially increased (3.58 fold; $p < 0.01$) in *Sw*-EtOH extract-treated A549 cells.

3.4. Sw-EtOH treatment efficiently inhibited the JAK1/STAT3 signaling pathway

Various studies have documented that JAK/STAT signaling pathway components are regarded as plausible therapeutic targets in several cancers, including lung cancer. It documented that prolonged activation of JAK/STAT signaling contributes to the malignancy of tumors by promoting its proliferation and survival,
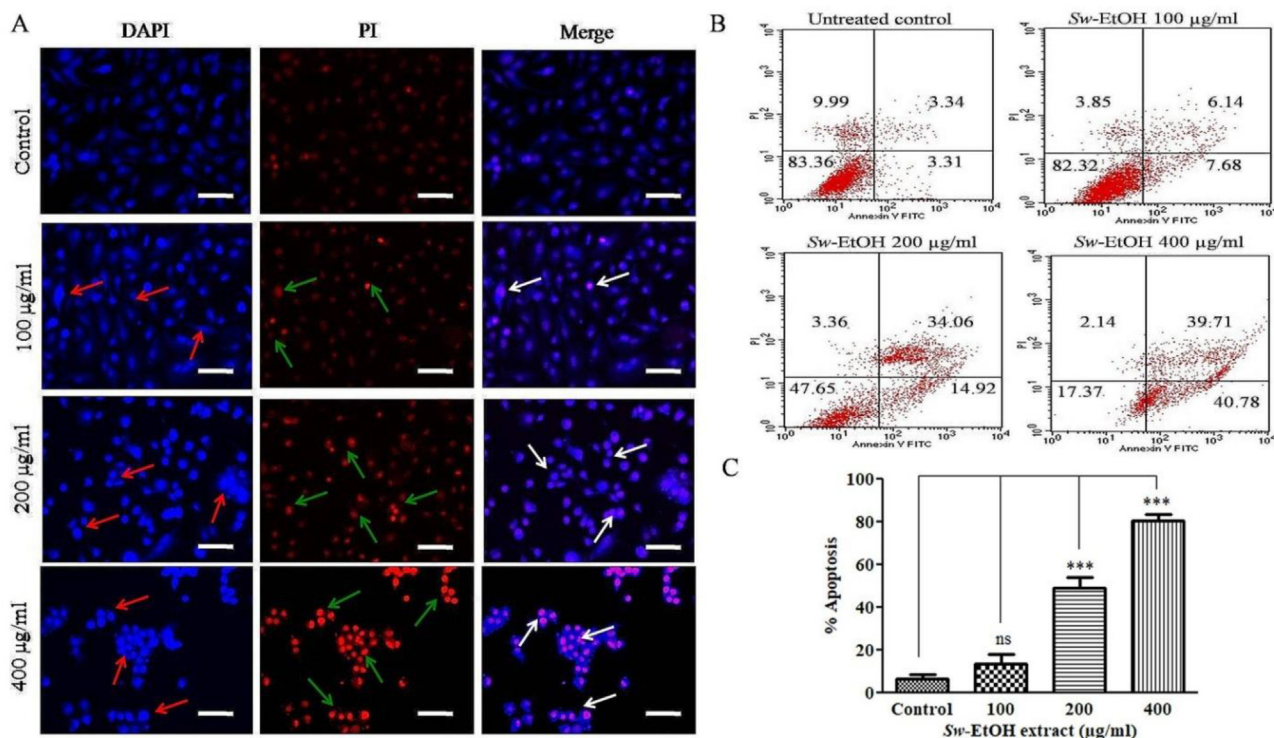
Fig. 3. (A) Sw-EtOH mediated induction of apoptosis within treated human lung cancer A549 cells. Increased levels of nuclear condensation and apoptosis are depicted within photomicrographs of vehicle control and Sw-EtOH treated (100–400 μg/ml) A549 cells stained with DAPI, P.I. and their merged fluorescence respectively indicated by red, green and white arrows. **(B)** Quantification of apoptosis percent (%) within A549 cells pre-treated Sw-EtOH for 24 h during Annexin V-FITC/PI. Early and late apoptotic cells were found to be stained in the lower right (L.R.) and the upper right (U.R.) quadrants respectively and **(C)** total percent apoptosis depicted as bar graph as evident during in Annexin V-FITC/PI assay. Data communicated constitutes the mean ± SEM of individual experiments performed thrice in triplicates. The level of significance among different Sw-EtOH treated groups was determined using one-way Anova and Dunnett post-hoc in comparison with untreated control where *represents $p < 0.05$, **$p < 0.01$ and ***$p < 0.001$; (Scale bar = 100 μm).

angiogenesis and immune evasion (Ahn et al., 2011). Thus, during our investigation, we focused on exploring the efficacy of Sw-EtOH extract on JAK1/STAT3 signaling pathway in A549 lung cancer cells. Our findings revealed that Sw-EtOH extract treatment inhibited JAK1/STAT3 pathway by deflating the expressional level of JAK1 mRNA and STAT3 mRNA in a dose-dependent manner. As observed, Sw-EtOH at concentrations of 100, 200 and 400 μg/ml reduced the gene expression level of JAK1 mRNA to 0.86 ± 0.11, 0.43 ± 0.16 and 0.32 ± 0.08 folds ($p < 0.05$) respectively, whereas expression of STAT3 mRNA was found to be 0.92 ± 0.03 (100 μg/ml), 0.52 ± 0.08 (200 μg/ml) and 0.42 ± 0.11 (400 μg/ml) folds ($p < 0.01$) in comparison with their respective control (Fig. 5A & B).

3.5. Sw-EtOH extract treatment modulated the expression of STAT3 coordinated survival proteins

3.5.1. Anti-apoptosis associated proteins

Previously, it has been established that constitutive expression of STAT3 promotes tumorigenesis by upregulating the gene expression level of certain anti-apoptotic proteins, primarily Bcl-xL, Bcl2 and Mcl1 in various solid carcinomas, including NSCLC (approximately 22% to 65%) (Yeh et al., 2013). Thus, we evaluated the efficacy of Sw-EtOH extract treatment on the gene expression level of the above-mentioned anti-apoptotic proteins. We found that anti-apoptotic markers' mRNA expression levels, namely Bcl-xL, Bcl2 and Mcl1 were substantially downregulated post-treatment with Sw-EtOH. The mRNA expression level of Bcl-xL, Bcl2 and Mcl1 were decreased to 0.92 ± 0.07, 0.63 ± 0.17 & 0.49 ± 0.14 fold; 0.90 ± 0.03, 0.58 ± 0.05 & 0.42 ± 0.11folds and 0.83 ± 0.16, 0.59 ± 0.25 & 0.34 ± 0.11folds ($p < 0.05$, $p < 0.01$ and $p < 0.01$)

respectively in a dose-dependent manner as shown in Fig. 5C, D, & E.

3.5.2. Proliferation related genes

Accumulating evidence has suggested that upstream regulators of STAT3 play an important role in lung cancer by increasing the expression of IL-6 in about 40% of patients (Demaria et al., 2012). After that, we investigated the efficacy of Sw-EtOH extract treatment on the gene expression of IL-6. We found that the mRNA expression levels of IL-6 were substantially downregulated after treatment with Sw-EtOH. The mRNA expression level of IL-6 decreased to 0.92 ± 0.20, 0.63 ± 0.15 & 0.32 ± 0.15 folds ($p < 0.001$) respectively in a dose-dependent manner as shown in Fig. 5F.

3.5.3. Cell cycle progression associated proteins

Aberrant activation of STAT3 mediates the overexpression of cell proliferation-associated proteins, namely cyclinD1 and c-myc, required for the tumor growth (Liang et al., 2011). We tried to decipher the effect of Sw-EtOH extract treatment on modulating the expression level of the above-mentioned proteins in A549 lung cancer cells. The results of qPCR analysis revealed that the mRNA expression level of cyclinD1 and c-myc decreased to 0.94 ± 0.16, 0.77 ± 0.15 & 0.31 ± 0.06 folds ($p < 0.05$) and 0.85 ± 0.11, 0.39 ± 0.13 & 0.10 ± 0.02 folds ($p < 0.01$) respectively (Fig. 6A & B).

3.5.4. Cell cycle arrest associated proteins

We performed qPCR analysis to investigate the efficacy of Sw-EtOH extract on cell cycle regulatory genes within Sw-EtOH treated A549 NSCLC cells. These results indicated that the mRNA expres-
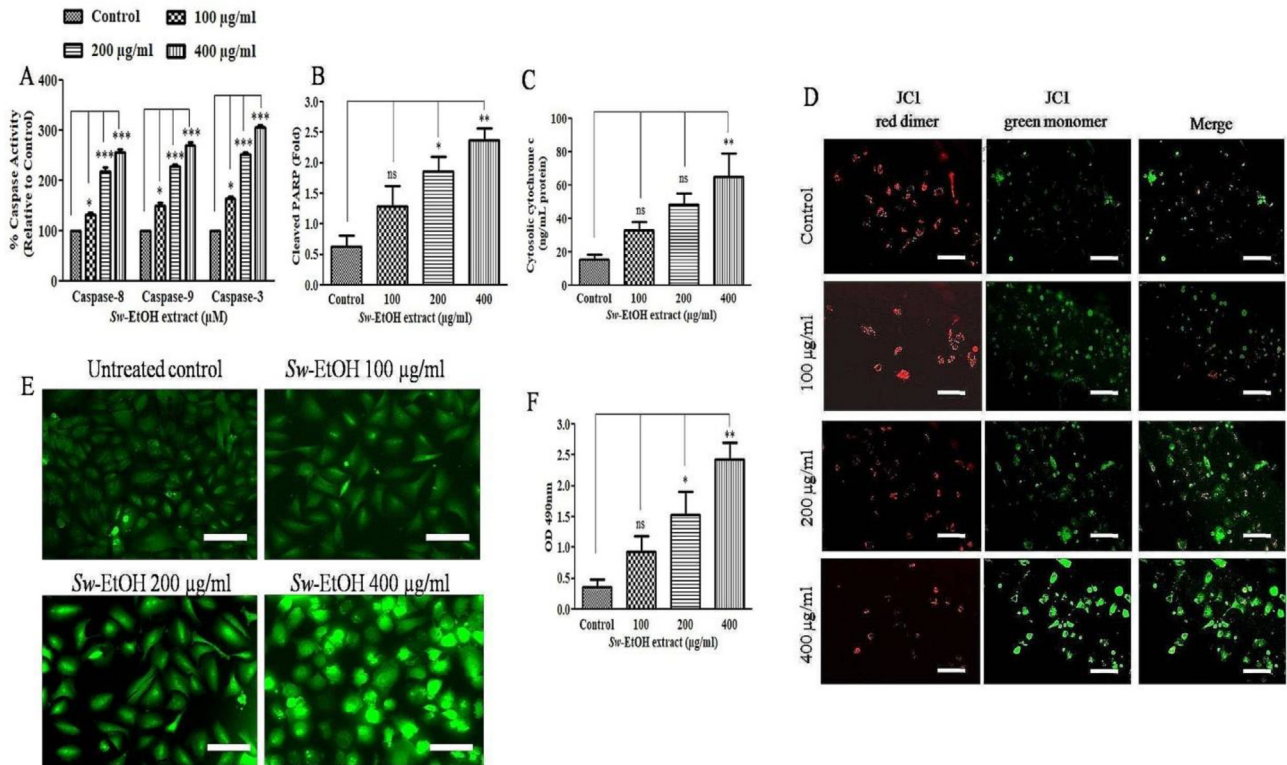
Fig. 4. Effects of *Sw*-EtOH on **(A)** caspase-3, -8 and -9 activities **(B)** cleaved PARP levels and **(C)** cytosolic cytochrome *c*. **(D)** Fluorescent micrographs showing disrupted mitochondrial membrane potential in JC-1-stained A549 cells after treatment with *Sw*-EtOH (100–400 µg/ml). **(E)** photomicrographs qualitatively elucidating augmented ROS levels within *Sw*-EtOH pre-treated A549 cells with different mentioned concentrations of *Sw*-EtOH for 6 h and subsequently stained with DCFH-DA **(F)** Quantification of 8-OHdG, a DNA damage marker, in A549 cells. Data communicated constitutes the mean ± SEM of individual experiments performed thrice in triplicates. The level of significance among different *Sw*-EtOH treated groups was determined using one-way Anova and Dunnett post-hoc in comparison with untreated control where *represents $p < 0.05$, **$p < 0.01$ and ***$p < 0.001$. (Scale bar = 100 µm).
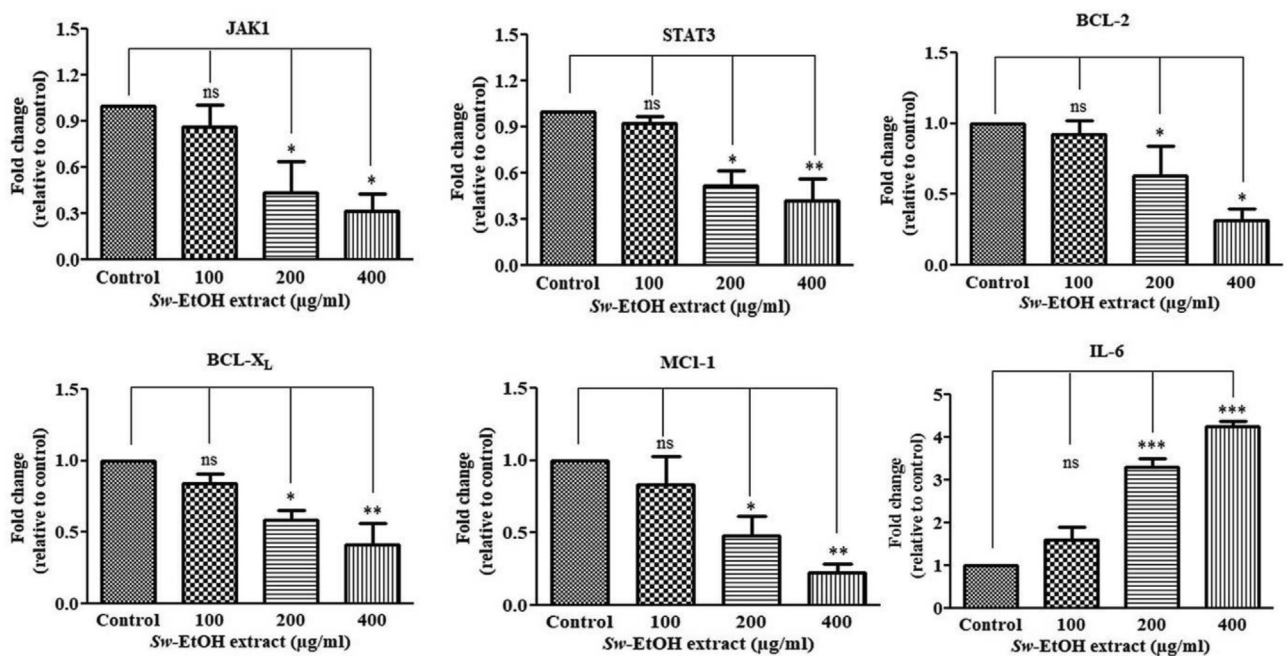

Fig. 5. *Sw*-EtOH mediated effect on mRNA expression of **(A)** JAK1 **(B)** STAT3 **(C)** Bcl-xL, **(D)** Bcl2 **(E)** Mcl1 and **(F)** IL- 6 genes. A549 cells were treated with 0–400 µg/ml for 24 h. Fold change in expression of all target genes was normalized to GAPDH mRNA which served as internal control. Data communicated constitutes the mean ± SEM of individual experiments performed thrice in triplicates. The level of significance among different *Sw*-EtOH treated groups was determined using one-way Anova and Dunnett post-hoc in comparison with untreated control where *represents $p < 0.05$, **$p < 0.01$ and ***$p < 0.001$.
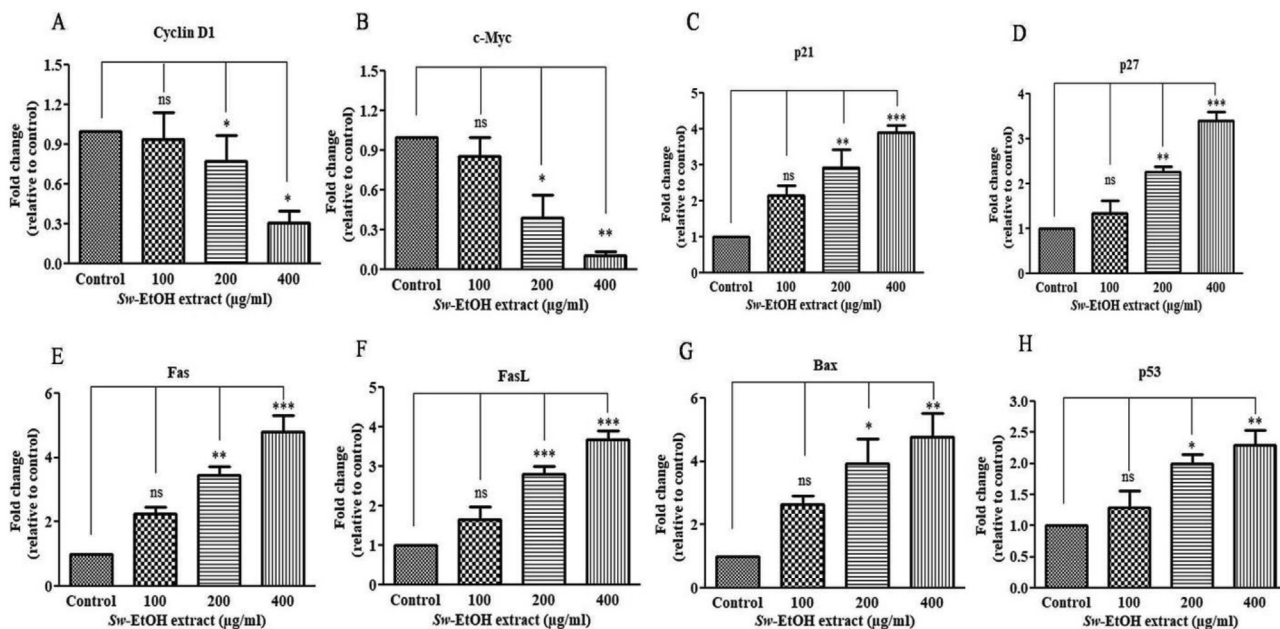
Fig. 6. *Sw*-EtOH induced alteration within the genes involved in cell cycle progression such as **(A)** cyclin D1, **(B)** c-Myc, **(C)** p21 **(D)** p27 and pro-apoptotic genes **(E)** Fas, **(F)** Fas-L, **(G)** Bax and **(H)** p53. Data communicated constitutes the mean ± SEM of individual experiments performed thrice in triplicates. The level of significance among different *Sw*-EtOH treated groups was determined using one-way Anova and Dunnett post-hoc in comparison with untreated control where *represents $p < 0.05$, **$p < 0.01$ and ***$p < 0.001$.

sion of p21 and p27 were significantly increased by 1.64 ± 0.26, 2.93 ± 0.39, 3.90 ± 0.16 ($p < 0.001$) folds and 1.33 ± 0.24, 2.26 ± 0.09, 2.73 ± 0.45 ($p < 0.01$) folds, respectively upon treatment with *Sw*-EtOH (Fig. 6C & D).

3.5.5. Apoptosis induction related proteins

It is reported that STAT3 activation mediates down regulation of important proteins such as P53, Fas, Fas-L and Bax involved in inducing apoptosis (Al Zaid Siddiquee and Turkson, 2008). To examine whether *Sw*-EtOH treatment could up regulate the expressional levels of these proteins, qPCR analysis was undertaken. Our findings found that the mRNA expression of P53, Fas, Fas-L and Bax increased by 1.10 ± 0.14, 1.99 ± 0.12 & 2.30 ± 0.18 ($p < 0.001$) folds; 2.24 ± 0.18, 3.46 ± 0.21 & 4.80 ± 0.42 ($p < 0.001$) folds; 1.65 ± 0.25, 2.79 ± 0.16 & 3.67 ± 0.18 ($p < 0.01$) folds and 2.65 ± 0.20, 3.93 ± 0.63 & 4.77 ± 0.61 ($p < 0.01$) folds respectively post *Sw*-EtOH extract treatment as shown in Fig. 6E, F, G & H.

4. Discussion

Many chemical constituents with propitious pharmacological activities have been identified from the extract of *S. chirayita* plant; however, such compounds have not been well characterized, specifically against the human application. The plant consists of a number of pharmaceutically important phytochemicals such as xanthones, ursolic acid, flavonoids, terpenoids, iridoids, amarogentin, glycosides, secoiridoids and swertiamarin (Khanal et al., 2015). The occurrence of transparent monoterpene alkaloid like Gentianine has also been reported in the extract of *S. chirayita*. It is soluble in an aqueous solution and well-known for its anti-inflammatory, anaesthetic, antihistamine, anticonvulsant properties (Lim et al., 2006). Further, swertiamarin, a secoiridoid glycoside present within the extract of this plant, is accountable for its analgesic property (Leong et al., 2016). Thus, the above-mentioned nutraceutical potential of this plant compels us to decipher its anticancer efficacy against lung cancer cells.

In our present research, we provide evidence that *Sw*-EtOH exerts antiproliferative and anticancer effects by growth inhibition, induction of apoptosis and altered expression of JAK1 and STAT3 associated proteins in A549 NSCLC cells to establish the possible implication of extract mediated inhibition of JAK1/STAT3 signaling pathway (He et al., 2017). We primarily determined the cytotoxic effect of *Sw*-EtOH on A549 NSCLC cells as it is a key step in evaluating the apoptotic potential of the targeted anticancer agent. Our findings based on MTT and LDH assays suggested that treatment of A549 NSCLC cells with *Sw*-EtOH extract blocked their proliferation, which was directly proportional to the different concentrations of *Sw*-EtOH. The morphological assessment further reaffirmed morphological alterations, including cellular shrinkage, membrane blebbing and cell detachment, which altogether indicates apoptosis in *Sw*-EtOH-treated A549 cells.

Induction of apoptosis by drugs has emerged as an efficient therapeutic intervention against cancer cells (Wu et al., 2019). DNA fragmentation and chromatin condensation are the prime characteristics of apoptosis, and these were observed in NSCLC cells post-treatment with *Sw*-EtOH. Moreover, the findings of the FITC-Annexin V/PI assay also confirmed the apoptotic potential of *Sw*-EtOH extract in A549 cells. It was found that *Sw*-EtOH substantially increased the percentage of Annexin-V positive cells in a dose-proportional manner in NSCLC A549 cells implicating that *Sw*-EtOH extract is an apoptotic agent.

Caspases are important members of the cysteine protease family and are an integral part of apoptotic pathways (Taylor et al., 2008). During apoptosis, their activation involves engagement of the death receptor pathway or extrinsic pathway where caspase-8 serves to be the initiator of this pathway and is activated by the TNF family, or via mitochondrial apoptotic pathway resulting in the release of cytochrome *c* (Nica et al., 2008). Both pathways eventually result in the subsequent cleavage and activation of major downstream effector protease such as caspase-3. In line with these observations, our study also elucidated that *Sw*-EtOH extract-induced apoptosis is accompanied by caspase activation, PARP cleavage, loss of Δψm, cytochrome *c* release, ROS generation,

increased 8-OHdG amount, upregulated expression of apoptotic proteins (Bax), reduced expression of anti-apoptotic proteins (Bcl-2, Bcl-XL & Mcl1) and increased expression of Fas and Fas-in NSCLC A549 cells. Thus, our data revealed that *Sw*-EtOH induces apoptosis via both intrinsic and extrinsic apoptosis pathways in NSCLC cells.

p53 also serves an important role in regulating tumor metasta-sis and invasion in NSCLC (Ahn et al., 2011). Consequently, activa-tion or gain of function by p53 may serve to be an effective therapeutic target in several carcinomas. Our present findings demonstrated that the treatment of *Sw*-EtOH extracts increased the functional expression of p53 and its downstream components such as p21 and p27 in A549 cells. Therefore, implicating that *Sw*-EtOH may also exert its anticancer activity by inducing the acti-vation of the p53 cascade.

Cyclin D1 is a member of the G1 cyclin family, which regulates G1–S transition during the cell cycle (Chiang et al., 2019) and is regarded as the most important checkpoint within the mammalian cell cycle (Motokura et al., 1991). Moreover, cyclin D1 mediates the phosphorylation and functional inactivation of retinoblastoma (R. B.) protein associated with cyclin-dependent kinases (CDK) such as CDK4 and CDK6. Earlier reports have shown that the overex-pression of cyclinD1 is involved in the development and progres-sion of NSCLCs. Our data demonstrated that *Sw*-EtOH extract effectively decreased the expressional levels of cycinD1 mRNA in A549 cells, indicating G1 phase arrest. c-Myc is yet another multi-functional oncogene involving cell growth, proliferation, tumorige-nesis, and therefore is found overexpressed in different carcinomas. One of the key biological functions of c-Myc is to pro-mote cell-cycle progression in several cancers. Interestingly, *Sw*-EtOH extract substantially downregulated the expression of c-Myc mRNA in A549 cells, demonstrating that inhibition of c-Myc post-Sw-EtOH treatment could be related to apoptosis induction and G1 phase arrest in NSCLCs.

JAK/STAT is also an important signaling pathway involved in tumorigenesis and found frequently dysregulated in diverse types of carcinomas (Sansone and Bromberg, 2012). Activated JAK/STAT leads to downstream activation of genes, namely cyclin D1, survivin and Bcl-2, which regulates cell proliferation and invasion and cell sur-vival (Sakamoto et al., 2007). Our study established that *Sw*-EtOH instigated the suppression of JAK1 mRNA within NSCLC cells.

Previous studies have established STAT3 as an important down-stream effector molecule of JAK/STAT signaling pathway. STAT3, a transcription factor, regulates the expression of various genes and consequently exerts its effects on several cellular processes such as growth, migration, apoptosis, and autophagy (Baxter et al., 2005). Constitutive phosphorylation of STAT3 correlates with cell prolifer-ation, resistance to chemotherapy and poor prognosis during lung carcinoma (Kralovics et al., 2005). We extended our interest in studying the potency of *Sw*-EtOH extract on the gene expression of STAT3 in treated A549 lung cancer cells. Our qPCR analysis sub-stantiated that *Sw*-EtOH extract treatment significantly downregu-lated the expression level of STAT3 mRNA in NSCLCs. Earlier, activation of STAT3 is known to enhance the expression level of key anti-apoptotic proteins, namely Mcl-1, Bcl-2 and Bcl-XL. These proteins are well-known for their role in enhancing the prolifera-tion of cancerous cells (Gao et al., 2005).

Furthermore, cyclin D1 and c-Myc have been reported to enhance the proliferation required for the tumor growth (Yokogami et al., 2013). Contrastingly, studies have also documented that STAT3 down-regulate the expression of several key such as p53, Fas, Fas-L and Bax involved in apoptosis induction (Niu et al., 2005). Therefore, we investigated the effect of *Sw*-EtOH extract on the expression level of STAT3 associated genes in NSCLCs.

Intriguingly, higher levels of IL-6 are found in the serum of advanced and metastatic cancer patients, including lung cancer patients (Scott et al., 1996). As a result, we inspected the effect of *Sw*-EtOH extract on the expression level of IL-6 in lung cancer cells. Our qPCR findings exhibited that *Sw*-EtOH extract downregulated IL-6 mRNA expression in a dose-dependent manner. In sum, it can be stated that *Sw*-EtOH extract suppresses JAK1/STAT3 signal-ing pathway and thereby induced apoptosis to obstruct the growth and viability of A549 NSCLCs. Taken together, *Sw*-EtOH extract holds the potential of being a plausible novel therapeutic for lung cancer; however, supporting in vivo and clinical exploration are still warranted.

5. Conclusions

In conclusion, our present findings indicated for the first time that *Sw*-EtOH extracts inhibited the JAK1/STAT3 signaling pathway and induce apoptosis via regulating the expression of apoptotic proteins such as BcL-2, Bcl-XL, Mcl-1, Fas, Fas-L, p53 & Bax along with modulating the expression of cyclin D1, c-Myc, p21 & p27 which would eventually halt the progression of the cell cycle. Thus, *Sw*-EtOH extract could be a potential agent for targeting NSCLC cells with constitutively activated JAK1/STAT3 signaling pathway owing to its ability to modulate STAT3 associated proteins, thereby presses the need for preclinical and clinical explorations of *Sw*-EtOH as an anticancer agent.

Declaration of Competing Interest

The authors declare that they have no known competing finan-cial interests or personal relationships that could have appeared to influence the work reported in this paper.

References

Ahmad, A., Ansari, I.A., 2020. Carvacrol Exhibits Chemopreventive Potential against Cervical Cancer Cells via Caspase-Dependent Apoptosis and Abrogation of Cell Cycle Progression. Anticancer Agents Med. Chem.

Ahmad, S., Khan, M.Y., Rafi, Z., Khan, H., Siddiqui, Z., Rehman, S., Shahab, U., Khan, M. S., Saeed, M., Alouffi, S., Khan, M.S., 2018. Oxidation, glycation and glycoxidation-The vicious cycle and lung cancer. Semin. Cancer Biol. 49, 29–36.

Ahn, H.J., Kim, K.I., Kim, G., Moon, E., Yang, S.S., Lee, J.S., 2011. Atmospheric-pressure plasma jet induces apoptosis involving mitochondria via generation of free radicals. PLoS ONE 6, e28154.

Al Zaid Siddiquee, K., Turkson, J., 2008. STAT3 as a target for inducing apoptosis in solid and hematological tumors. Cell Res. 18, 254–267.

Baxter, E.J., Scott, L.M., Campbell, P.J., East, C., Fourouclas, N., Swanton, S., Vassiliou, G.S., Bench, A.J., Boyd, E.M., Curtin, N., Scott, M.A., Erber, W.N., Green, A.R., Cancer Genome, P., 2005. Acquired mutation of the tyrosine kinase JAK2 in human myeloproliferative disorders. Lancet 365, 1054–1061.

Chen, X.M., Bai, Y., Zhong, Y.J., Xie, X.L., Long, H.W., Yang, Y.Y., Wu, S.G., Jia, Q., Wang, X.H., 2013. Wogonin has multiple anti-cancer effects by regulating c-Myc/SKP2/ Fbw7alpha and HDAC1/HDAC2 pathways and inducing apoptosis in human lung adenocarcinoma cell line A549. PLoS ONE 8, e79201.

Chiang, S.R., Lin, C.S., Lin, H.H., Shieh, P.C., Kao, S.H., 2019. Bergapten induces G1 arrest of nonsmall cell lung cancer cells, associated with the p53mediated cascade. Mol. Med. Rep. 19, 1972–1978.

Cui, J., Placzek, W.J., 2016. PTBP1 modulation of MCL1 expression regulates cellular apoptosis induced by antitubulin chemotherapeutics. Cell Death Differ. 23, 1681–1690.

Darnell Jr., J.E., Kerr, I.M., Stark, G.R., 1994. Jak-STAT pathways and transcriptional activation in response to IFNs and other extracellular signaling proteins. Science 264, 1415–1421.

Demaria, M., Misale, S., Giorgi, C., Miano, V., Camporeale, A., Campisi, J., Pinton, P., Poli, V., 2012. STAT3 can serve as a hit in the process of malignant transformation of primary cells. Cell Death Differ. 19, 1390–1397.

Dutta, P., Sabri, N., Li, J., Li, W.X., 2014. Role of STAT3 in lung cancer. JAKSTAT 3, e999503.

Gao, L.F., Xu, D.Q., Wen, L.J., Zhang, X.Y., Shao, Y.T., Zhao, X.J., 2005. Inhibition of STAT3 expression by siRNA suppresses growth and induces apoptosis in laryngeal cancer cells. Acta Pharmacol. Sin. 26, 377–383.

He, Q.-Y., Wang, R., Sun, X.-C., 2017. Cytotoxicity of methanolic extract of Swertia petiolata against gastric cancer cell line SNU-5 is via induction of apoptosis. S. Afr. J. Bot. 109, 196–202.

Jin, W., 2020. Role of JAK/STAT3 Signaling in the Regulation of Metastasis, the Transition of Cancer Stem Cells, and Chemoresistance of Cancer by Epithelial-Mesenchymal Transition. Cells 9.

Karagul, M.I., Aktas, S., Yilmaz, S.N., Yetkin, D., Celikcan, H.D., Cevik, O.S., 2020. Perifosine and vitamin D combination induces apoptotic and non-apoptotic cell death in endometrial cancer cells. EXCLI J. 19, 532–546.

Kaushik, N., Lee, S.J., Choi, T.G., Baik, K.Y., Uhm, H.S., Kim, C.H., Kaushik, N.K., Choi, E. H., 2015. Non-thermal plasma with 2-deoxy-D-glucose synergistically induces cell death by targeting glycolysis in blood cancer cells. Sci. Rep. 5, 8726.

Khanal, S., Shakya, N., Thapa, K., Pant, D.R., 2015. Phytochemical investigation of crude methanol extracts of different species of Swertia from Nepal. BMC Res. Notes 8, 821.

Kralovics, R., Passamonti, F., Buser, A.S., Teo, S.S., Tiedt, R., Passweg, J.R., Tichelli, A., Cazzola, M., Skoda, R.C., 2005. A gain-of-function mutation of JAK2 in myeloproliferative disorders. N. Engl. J. Med. 352, 1779–1790.

Kumar, V., Van Staden, J., 2015. A Review of Swertia chirayita (Gentianaceae) as a Traditional Medicinal Plant. Front. Pharmacol. 6, 308.

LaFave, L.M., Levine, R.L., 2012. JAK2 the future: therapeutic strategies for JAK-dependent malignancies. Trends. Pharmacol. Sci. 33, 574–582.

Lee, J., Jang, H.J., Chun, H., Pham, T.H., Bak, Y., Shin, J.W., Jin, H., Kim, Y.I., Ryu, H.W., Oh, S.R., Yoon, D.Y., 2019. Calotropis gigantea extract induces apoptosis through extrinsic/intrinsic pathways and reactive oxygen species generation in A549 and NCI-H1299 non-small cell lung cancer cells. BMC Complement Altern. Med. 19, 134.

Leong, X.Y., Thanikachalam, P.V., Pandey, M., Ramamurthy, S., 2016. A systematic review of the protective role of swertiamarin in cardiac and metabolic diseases. Biomed. Pharmacother. 84, 1051–1060.

Liang, Z.W., Guo, B.F., Li, Y., Li, X.J., Li, X., Zhao, L.J., Gao, L.F., Yu, H., Zhao, X.J., Zhang, L., Yang, B.X., 2011. Plasmid-based Stat3 siRNA delivered by hydroxyapatite nanoparticles suppresses mouse prostate tumour growth in vivo. Asian J. Androl. 13, 481–486.

Lim, H., Son, K.H., Chang, H.W., Kang, S.S., Kim, H.P., 2006. Inhibition of chronic skin inflammation by topical anti-inflammatory flavonoid preparation, Ato Formula. Arch Pharm. Res. 29, 503–507.

Lin, M.X., Lin, S.H., Li, Y.R., Chao, Y.H., Lin, C.H., Su, J.H., Lin, C.C., 2017. Lobocrassin B Induces Apoptosis of Human Lung Cancer and Inhibits Tumor Xenograft Growth. Mar. Drugs 15.

Medeiros, L.J., Hai, S., Thomazy, V.A., Estalilla, O.C., Romaguera, J., Luthra, R., 2002. Real-time RT-PCR assay for quantifying cyclin D1 mRNA in B-cell non-Hodgkin's lymphomas. Mod. Pathol. 15, 556–564.

Motokura, T., Bloom, T., Kim, H.G., Juppner, H., Ruderman, J.V., Kronenberg, H.M., Arnold, A., 1991. A novel cyclin encoded by a bcl1-linked candidate oncogene. Nature 350, 512–515.

Nica, A.F., Tsao, C.C., Watt, J.C., Jiffar, T., Kurinna, S., Jurasz, P., Konopleva, M., Andreeff, M., Radomski, M.W., Ruvolo, P.P., 2008. Ceramide promotes apoptosis in chronic myelogenous leukemia-derived K562 cells by a mechanism involving caspase-8 and JNK. Cell Cycle 7, 3362–3370.

Niu, G., Wright, K.L., Ma, Y., Wright, G.M., Huang, M., Irby, R., Briggs, J., Karras, J., Cress, W.D., Pardoll, D., Jove, R., Chen, J., Yu, H., 2005. Role of Stat3 in regulating p53 expression and function. Mol. Cell. Biol. 25, 7432–7440.

Rego, D., Kumar, A., Nilchi, L., Wright, K., Huang, S., Kozlowski, M., 2011. IL-6 production is positively regulated by two distinct Src homology domain 2-containing tyrosine phosphatase-1 (SHP-1)-dependent CCAAT/enhancer-binding protein beta and NF-kappaB pathways and an SHP-1-independent NF-kappaB pathway in lipopolysaccharide-stimulated bone marrow-derived macrophages. J. Immunol. 186, 5443–5456.

Sakamoto, K., Creamer, B.A., Triplett, A.A., Wagner, K.U., 2007. The Janus kinase 2 is required for expression and nuclear accumulation of cyclin D1 in proliferating mammary epithelial cells. Mol. Endocrinol. 21, 1877–1892.

Sansone, P., Bromberg, J., 2012. Targeting the interleukin-6/Jak/stat pathway in human malignancies. J. Clin. Oncol. 30, 1005–1014.

Scott, H.R., McMillan, D.C., Crilly, A., McArdle, C.S., Milroy, R., 1996. The relationship between weight loss and interleukin 6 in non-small-cell lung cancer. Br. J. Cancer 73, 1560–1562.

Shamloo, B., Usluer, S., 2019. p21 in Cancer Research. Cancers (Basel) 11.

Sun, H., Yin, M., Hao, D., Shen, Y., 2020. Anti-Cancer Activity of Catechin against A549 Lung Carcinoma Cells by Induction of Cyclin Kinase Inhibitor p21 and Suppression of Cyclin E1 and P-AKT. Appl. Sci. 10, 2065.

Taga, T., Hibi, M., Hirata, Y., Yamasaki, K., Yasukawa, K., Matsuda, T., Hirano, T., Kishimoto, T., 1989. Interleukin-6 triggers the association of its receptor with a possible signal transducer, gp130. Cell 58, 573–581.

Tao, Y., Zhou, X., Liu, Z., Zhang, X., Nie, Y., Zheng, X., Li, S., Hu, X., Yang, G., Zhao, Q., Mou, C., 2020. Expression patterns of three JAK-STAT pathway genes in feather follicle development during chicken embryogenesis. Gene Expr. Patterns 35, 119078.

Taylor, R.C., Cullen, S.P., Martin, S.J., 2008. Apoptosis: controlled demolition at the cellular level. Nat. Rev. Mol. Cell Biol. 9, 231–241.

Tiwari, R.K., Chandrakar, P., Gupta, C.L., Sayyed, U., Shekh, R., Bajpai, P., 2021. Leishmanial CpG DNA nanovesicles: A propitious prophylactic approach against visceral leishmaniasis. Int. Immunopharmacol. 90, 107181.

Wang, S., Han, X., Zhang, L., Zhang, Y., Li, H., Jiao, Y., 2018. Whole Peptidoglycan Extracts from the Lactobacillus paracasei subsp. paracasei M5 Strain Exert Anticancer Activity In Vitro. Biomed. Res. Int. 2018, 2871710.

Wu, D., Wang, Z., Lin, M., Shang, Y., Wang, F., Zhou, J., Wang, F., Zhang, X., Luo, X., Huang, W., 2019. In Vitro and In Vivo Antitumor Activity of Cucurbitacin C, a Novel Natural Product From Cucumber. Front. Pharmacol. 10, 1287.

Yang, C.L., Liu, Y.Y., Ma, Y.G., Xue, Y.X., Liu, D.G., Ren, Y., Liu, X.B., Li, Y., Li, Z., 2012. Curcumin blocks small cell lung cancer cells migration, invasion, angiogenesis, cell cycle and neoplasia through Janus kinase-STAT3 signalling pathway. PLoS ONE 7, e37960.

Yeh, C.T., Huang, W.C., Rao, Y.K., Ye, M., Lee, W.H., Wang, L.S., Tzeng, D.T., Wu, C.H., Shieh, Y.S., Huang, C.Y., Chen, Y.J., Hsiao, M., Wu, A.T., Yang, Z., Tzeng, Y.M., 2013. A sesquiterpene lactone antrocin from Antrodia camphorata negatively modulates JAK2/STAT3 signaling via microRNA let-7c and induces apoptosis in lung cancer cells. Carcinogenesis 34, 2918–2928.

Yokogami, K., Yamashita, S., Takeshima, H., 2013. Hypoxia-induced decreases in SOCS3 increase STAT3 activation and upregulate VEGF gene expression. Brain Tumor. Pathol. 30, 135–143.

Yu, H., Lee, H., Herrmann, A., Buettner, R., Jove, R., 2014. Revisiting STAT3 signalling in cancer: new and unexpected biological functions. Nat. Rev. Cancer 14, 736–746.

Yuan, M., Huang, L.L., Chen, J.H., Wu, J., Xu, Q., 2019. The emerging treatment landscape of targeted therapy in non-small-cell lung cancer. Signal Transduct. Target Ther. 4, 61.

Zappa, C., Mousa, S.A., 2016. Non-small cell lung cancer: current treatment and future advances. Transl Lung Cancer Res. 5, 288–300.

Zhao, G., Zhu, G., Huang, Y., Zheng, W., Hua, J., Yang, S., Zhuang, J., Ye, J., 2016. IL-6 mediates the signal pathway of JAK-STAT3-VEGF-C promoting growth, invasion and lymphangiogenesis in gastric cancer. Oncol. Rep. 35, 1787–1795.

Zucchini, N., de Sousa, G., Bailly-Maitre, B., Gugenheim, J., Bars, R., Lemaire, G., Rahmani, R., 2005. Regulation of Bcl-2 and Bcl-xL anti-apoptotic protein expression by nuclear receptor PXR in primary cultures of human and rat hepatocytes. Biochim. Biophys. Acta, Mol. Cell. Biol. Lipids 1745, 48–58.